

This article was downloaded by: [University Of Maryland]

On: 28 August 2013, At: 11:23

Publisher: Taylor & Francis

Informa Ltd Registered in England and Wales Registered Number: 1072954 Registered office: Mortimer House, 37-41 Mortimer Street, London W1T 3JH, UK



Aerosol Science and Technology

Publication details, including instructions for authors and subscription information:

<http://www.tandfonline.com/loi/uast20>

Evaluating the Mobility of Nanorods in Electric Fields

Mingdong Li^{a b c}, Rian You^{a b c}, George W. Mulholland^{a b c} & Michael R. Zachariah^{a b c}

^a Department of Chemical and Biomolecular Engineering, University of Maryland, College Park, Maryland, USA

^b Department of Chemistry and Biochemistry, University of Maryland, College Park, Maryland, USA

^c National Institute of Standards and Technology, Gaithersburg, Maryland, USA

Accepted author version posted online: 27 Jun 2013. Published online: 06 Aug 2013.

To cite this article: Mingdong Li, Rian You, George W. Mulholland & Michael R. Zachariah (2013) Evaluating the Mobility of Nanorods in Electric Fields, *Aerosol Science and Technology*, 47:10, 1101-1107, DOI: [10.1080/02786826.2013.819565](https://doi.org/10.1080/02786826.2013.819565)

To link to this article: <http://dx.doi.org/10.1080/02786826.2013.819565>

PLEASE SCROLL DOWN FOR ARTICLE

Taylor & Francis makes every effort to ensure the accuracy of all the information (the "Content") contained in the publications on our platform. However, Taylor & Francis, our agents, and our licensors make no representations or warranties whatsoever as to the accuracy, completeness, or suitability for any purpose of the Content. Any opinions and views expressed in this publication are the opinions and views of the authors, and are not the views of or endorsed by Taylor & Francis. The accuracy of the Content should not be relied upon and should be independently verified with primary sources of information. Taylor and Francis shall not be liable for any losses, actions, claims, proceedings, demands, costs, expenses, damages, and other liabilities whatsoever or howsoever caused arising directly or indirectly in connection with, in relation to or arising out of the use of the Content.

This article may be used for research, teaching, and private study purposes. Any substantial or systematic reproduction, redistribution, reselling, loan, sub-licensing, systematic supply, or distribution in any form to anyone is expressly forbidden. Terms & Conditions of access and use can be found at <http://www.tandfonline.com/page/terms-and-conditions>



Evaluating the Mobility of Nanorods in Electric Fields

Mingdong Li,^{1,2,3} Rian You,^{1,2,3} George W. Mulholland,^{1,2,3}
and Michael R. Zachariah^{1,2,3}

¹Department of Chemical and Biomolecular Engineering, University of Maryland, College Park, Maryland, USA

²Department of Chemistry and Biochemistry, University of Maryland, College Park, Maryland, USA

³National Institute of Standards and Technology, Gaithersburg, Maryland, USA

The mobility of a nonspherical particle is a function of both particle shape and orientation. In turn, the higher magnitude of electric field causes nonspherical particles to align more along the field direction, increasing their mobility or decreasing their mobility diameter. In previous works, Li et al. developed a general theory for the orientation-averaged mobility and the dynamic shape factor applicable to any axially symmetric particles in an electric field, and applied it to the specific cases of nanowires and doublets of spheres. In this work, the theory for a nanowire is compared with experimental results of gold nanorods with known shape determined by TEM images. We compare the experimental measured mobility sizes with the theoretical predicted mobility in the continuum, free molecular, and the transition regime. The mobility size shift trends in the electric fields based on our model, expressed both in the free molecular regime and in the transition regime, are in good agreement with the experimental results. For rods of dimension: width $d_r = 17$ nm and length $L_r = 270$ nm, where one length scale is smaller than the mean free path and one larger, the results clearly show that the flow regime of a slender rod is mostly controlled by the diameter of the rod (i.e., the smallest dimension). In this case, the free molecule transport properties best represented our nanorod. Combining both theory and experiment we show how, by evaluating the mobility as a function of applied electric field, we can extract both rod length and diameter.

1. INTRODUCTION

Most “real” particles encountered or manufactured are aspherical. In some cases, the nonspherical shape offers some

unique physical and chemical properties (e.g., nanowires), while in others, fractal structures comprising the particle are assemblies of near-spherical smaller particles (e.g., soot aggregates) and possess nontrivial transport, optical, and physical properties. One common method employed to characterize the dimensionality of particles regardless of shape is mobility.

As a general rule, by convenience particle mobility is usually expressed as an equivalent spherical diameter, (i.e., electrical mobility diameter) regardless of the actual particle shape. As such this measured analyte electrical mobility diameter represents the diameter of a sphere with that equivalent mobility. For a spherical particle, the electrical mobility diameter is equivalent to its geometric diameter. However, for an aspherical particle, the measured electrical mobility diameter is a function of both particle shape and particle orientation.

Song et al. (2005) demonstrated the effect of shape on particle mobility by transforming gold rods into near spheres and measuring the particle mobility diameters. They reported that the gold particle mobility diameters decreased from 55 to 25 nm. By creating doubles of spheres other researchers have shown that particle orientation (alignment) and thus mobility is a function of field intensity (Kousaka et al. 1996; Zelenyuk and Imre 2007). In a prior work, we were able to measure the length of carbon nanotubes by accounting for the electric field induced alignment effect (Kim et al. 2007; Li et al. 2012).

The theoretical evaluation of mobility relies on the expressions of the drag force, which is very well defined for spheres in all three regimes, free molecular, continuum, and the transition regimes. (Hinds 1999; Li and Wang 2003), but not as well defined for aspherical particles.

For the continuum regime, Dahneke (1973a) and Kasper et al. (1985) reviewed the drag force expressions for several symmetric shapes: ellipsoids, cylinders, discs, and cubes. The continuum drag forces on bodies of arbitrary shape with random orientations have also been proposed, including Kirkwood and Riseman (1948) and Hubbard and Douglas (1993). In the free molecular regime, Dahneke (1973b) provided a general integral expression for the drag force on a convex particle, and obtained

Received 24 April 2013; accepted 4 June 2013.

The authors thank Ranganathan Gopalakrishnan and Professor Christopher J. Hogan for providing us the vendor information for the gold nanorod colloid. Commercial equipment, instruments, or materials identified in this report does not imply recommendation or endorsement by the University of Maryland or the National Institute of Standards and Technology.

Address correspondence to Michael R. Zachariah, Department of Chemical and Biomolecular Engineering and Department of Chemistry and Biochemistry, University of Maryland, 2125 Martin Hall, College Park, MD 20742, USA. E-mail: mrz@umd.edu

specific expressions for several symmetric shapes, including: ellipsoids, cylinders discs, and cubes. Chan and Dakneke (1981) proposed a numerical technique to calculate the free-molecule drag on straight chains of uniform spheres. Mackowski (2006) also examined the hydrodynamic drag of fractal-like aggregates of spheres in the free-molecular flow regime using a Monte Carlo method. In the free-molecule regime, the orientationally averaged drag for arbitrarily shaped particles has been computed using cross-section approaches (Mason and McDaniel 1988), such as the exact hard-spheres scattering cross-section (EHSS) (Shvartsburg and Jarrold 1996) and projected area (PA) (von Helden et al. 1993) methods (strictly speaking, the PA approach is derived only for particles with a convex shape [Shvartsburg and Jarrold 1996; Li 2012]). For particles in the transition regime, Dahneke (1973c) proposed a scaling approach using an adjusted spherical diameter defined as proportional to the ratio of the free molecule drag to the continuum drag (Cheng 1991; Li et al. 2012). Zhang et al. (2012) applied an approach to aggregates in the transition regime, equivalent to Daneke's adjusted spherical diameter by using PA expression for the free-molecule drag, and employing the Hubbard and Douglas expression for the continuum drag.

However, all of these approaches only apply to particles traveling along a fixed direction, or moving when orientations follow a random distribution, and do not consider particle orientations following a nonrandom distribution due to some external force, such an electric force.

In our previous work (Li et al. 2012), we employed a tensor formulation of the drag force when computing the orientation-averaged mobility of axially symmetric particles using a Boltzmann probability distribution for the orientation. This model (requires information on the friction coefficient tensor) has been further extended to any particle shape in a systematic study of the mobility of nonspherical particles (Li 2012). Recently, this approach was validated by experimental results of well-defined doublets of NIST traceable size standard 127, 150, 200, and 240 nm PSL spheres (Li et al. 2013).

In this work, we employ well-defined monodisperse gold nanorods for which we show significant shifts in the measured mobility diameter with applied electric field. We then evaluate the resulting shift, in the context of our tensor model in both the free molecule and transition regime. Finally, we demonstrate that, by evaluating mobility as a function of applied electric field, both rod length and diameter can be determined from experimental mobility measurements.

2. MATERIALS AND EXPERIMENTAL METHODS

To evaluate particle alignment, it is necessary to obtain very well defined source material in an unaggregated state suitable for electrospray (ES)—differential mobility analysis (DMA). Such sources were not readily available, however, we are able to source suitable materials of colloidal gold (Nanopartz Inc.; MUTAB coated conjugated gold nanorods; 10 nm, SPR = 2000 nm, 0.25 mg, 1 mL; C12N-10-2000-TMU-0.25).

The colloidal solution was aerosolized using a 40- μm inner diameter capillary mounted in an electrospray aerosol generator (TSI Inc., Model 3480) with a neutralizer to provide a bipolar charge distribution to the particles. The neutralized particles were then passing through a nano (TSI Inc., Model 3085) or long DMA (TSI Inc., Model 3081) for particle mobility selection, and counted with an ultrafine condensed particle counter (CPC) (TSI Inc., Model 3025A). More details on the measurement method can be found in Li et al. (2011a,b) and Guha et al. (2012).

The mobility distribution was measured with different sheath flow rates ranging from $0.833 \times 10^{-4} \text{ m}^3/\text{s}$ (5 L/min) to $2.5 \times 10^{-4} \text{ m}^3/\text{s}$ (15 L/min) for a long DMA, and ranging from $0.5 \times 10^{-4} \text{ m}^3/\text{s}$ (3 L/min) to $1.667 \times 10^{-4} \text{ m}^3/\text{s}$ (10 L/min) for a nano DMA to enable a mobility measurement to be conducted on a monodisperse particle over a wide range of electric fields. The field strength in this work spans from 470 to 6775 volts/cm. All ratios of the sheath to aerosol flow exceeded 20 to guarantee suitably high size resolution. To avoid the effects of time varying electric field as the particles go thru the DMA, we operated the DMA in the step mode, and kept the step sufficiently long to ensure a complete transit through the DMA system before the voltage was changed (up to 45 s).

The mobility sizes of the gold nanorod was calibrated using 100.7 nm NIST standard reference material (PSL sphere) under the same experimental conditions of sheath flows at $0.833 \times 10^{-4} \text{ m}^3/\text{s}$ (5 L/min) and $2.5 \times 10^{-4} \text{ m}^3/\text{s}$ (15 L/min) with a long DMA, and sheath flows at $0.5 \times 10^{-4} \text{ m}^3/\text{s}$ (3 L/min) and $0.833 \times 10^{-4} \text{ m}^3/\text{s}$ (5 L/min) with a nano DMA, and using $60.6 \pm 0.2 \text{ nm}$ PSL spheres for sheath flows at $1.333 \times 10^{-4} \text{ m}^3/\text{s}$ (8 L/min) and $1.667 \times 10^{-4} \text{ m}^3/\text{s}$ (10 L/min) with a nano DMA. The mobility size of this $60.6 \pm 0.2 \text{ nm}$ PSL spheres was calibrated by 100.7 nm NIST standard reference material (PSL sphere) in a separate measurement. The measurements with the standard reference material (100.7 nm), $60.6 \pm 0.2 \text{ nm}$ PSL sphere and the gold nanorod were repeated three times respectively, and the assignment of DMA detection voltage was obtained by averaging the three means of the Gaussian fits to the experimental profile. The exact sheath flow value was assigned by measurement of the 100.7 nm NIST standard reference material, or the $60.6 \pm 0.2 \text{ nm}$ PSL sphere at the same condition as the gold nanorod measurement. Using this calibrated sheath flow value, the mobility sizes of the gold rod could be determined. The combined uncertainty for mobility sizes are based on three repeat voltage scans, the 0.47% uncertainty in the 100.7 nm calibration standard, and the flow rate calibration using 100.7 nm standard reference material ($\sim 0.2 \text{ nm}$) and has a nominal value of $\sim 0.55 \text{ nm}$.

3. RESULTS AND DISCUSSIONS

In this section, the experimental results on the effect of electric field on mobility are presented for the gold nanorods. The length and width distributions of the nanorods are characterized by TEM. The measured results for the alignment of singly charged rod particles are compared with our theoretical model

(Li et al. 2012). For the calculations of drag friction coefficients along the two principal directions, axial and radial, of a rod, we use two expressions: (a) Dahneke's drag force expression for a rod in the free molecular regime and (b) Dahneke's scaling approach (i.e., adjusted spherical diameter) for a rod in the transition regime. This was done because for the rods employed in our experiment, the diameter is smaller than the mean free path, while the length was larger.

3.1. TEM Dimensional Analysis

To evaluate the dimensions of the Au rod, TEM images were obtained from air dried samples of liquid dropped directly onto the TEM grid. Figures 1a and c show a TEM image and the processed results of 240 rods for rod length. To evaluate the length and width accurately enough to validate a mobility theory, it became necessary to calibrate the TEM images *in-situ* using the gold nanorods themselves from the very well know lattice space (inter-plane distance of $(\bar{1}\bar{1}\bar{1}) = 0.2355$ nm) for Au crystals as shown in Figure 1b. With this calibration, the length and width of our gold rods measured by TEM has an uncertainty of $\sim 4\%$.

This gold rod sample was also imaged after electrospray (ES) and mobility size selected at the peak voltage 5530 volts, which corresponds to the mobility size of ~ 67 nm at a sheath flow rate $\sim 1.333 \times 10^{-4}$ m³/s (8 L/min) and aerosol flow rate $\sim 0.117 \times 10^{-4}$ m³/s (0.7 L/min) using a commercial nano-DMA. Figure 2a and b show processed results of 30 rods, for rod length and width. These results are consistent with the histogram of length from a liquid droppered result of Figure 1. For our subsequent calculation we consider the diameter $d_r = 17$ nm and length $L_r = 270$ nm, based on the TEM images for our subsequent theoretical calculations.

3.2. The Effect of Electric Field on the Mobility of Rods

In Figure 3, we present two mobility size distributions of the gold rod sample at two different sheath flow rates, $Q_{sh} = 0.5 \times 10^{-4}$ m³/s (3 L/min), and 1.667×10^{-4} m³/s (10 L/min), in a nano DMA corresponding to two different magnitudes of electric field. Clearly then the measured mobility of these monodisperse nanorods is unambiguously electric field dependent. In Figure 4, we show the measured mobility diameters of the gold rods versus the applied electric fields. In this analysis, we regard mobility as a constant corresponding to an electric field equal to the electrode voltage divided by the radial distance between the two electrodes. In our previous work (Li et al. 2013), it was shown that the radial variation in the electric field affects the value of the mobility by less than 0.7%. For each measurement, the mobility size is calibrated using 100.7 nm PSL spherical particle (NIST standard reference material) or 60.6 nm PSL spherical particle whose size was calibrated using the 100.7 PSL reference sphere in a separate measurement. The variation of measured mobility diameter for the rods in Figure 3 shows that the effect of electric field induced alignment, which results in smaller mobility diameters (i.e., higher mobility) with higher

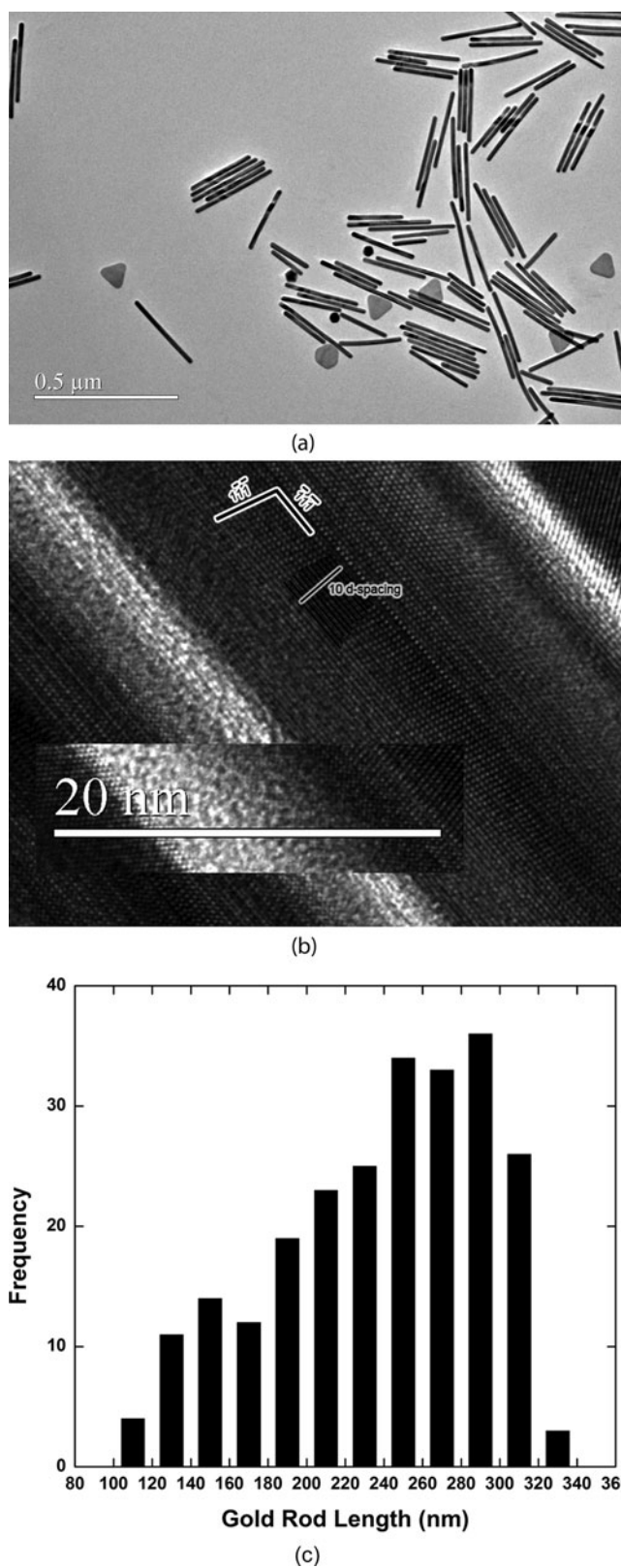


FIG. 1. (a) TEM image of the gold nanorod sample. (b) Gold lattice spacing are used for the calibrations of the length and width of gold rods. (c) Histogram of rod length of the gold nanorod sample.

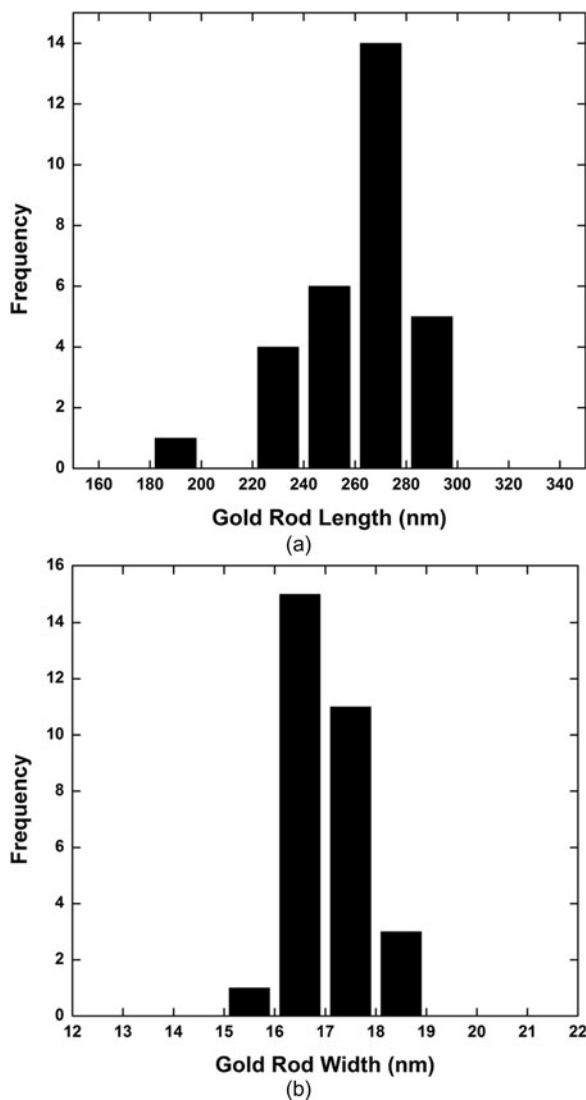


FIG. 2. (a) Histogram of the rod length of the gold nanorod sample after electro spray (ES) mobility size selection at a peak voltage 5530 volts, which corresponds to mobility size ~ 67 nm at a sheath flow rate $\sim 1.333 \times 10^{-4}$ m^3/s (8 L/min), and aerosol flow rate $\sim 0.117 \times 10^{-4}$ m^3/s (0.7 L/min) using a nano-DMA. (b) Histogram of the rod width of the size selected gold nanorod sample.

electric fields, is quite significant, with the mobility size shifting from 73.7 to 65.3 nm between low (470 volts/cm) and high electric fields (6775 volts/cm). Higher electric fields result in more alignment and a lower drag, thus increasing mobility, and decreasing the mobility diameter.

In the absence of Brownian forces, a wire would in an electric field align perfectly to lower its potential energy. Brownian dynamics however operates to randomize the orientation of the rod. For sufficiently small particles, over the time scale of interest, the rotational Brownian motion will result in a steady-state distribution of the orientation, i.e., Boltzmann angular distribution (Li 2012; Li et al. 2012, 2013). This angular distribution

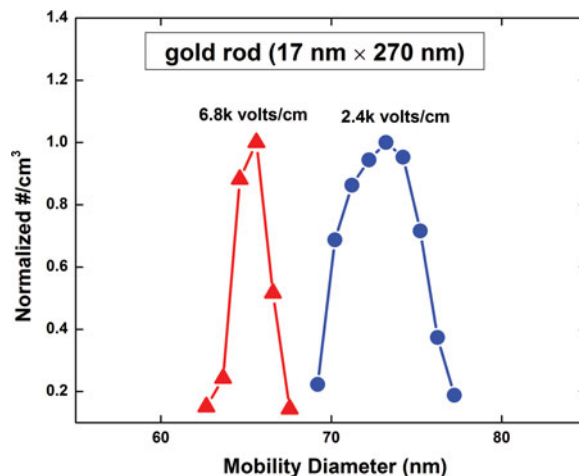


FIG. 3. Two mobility size distributions for the same monodisperse gold nanorods, measured at 0.5×10^{-4} m^3/s (3 L/min), and 1.667×10^{-4} m^3/s (10 L/min) sheath flow rates in a step mode nano DMA. The mobility diameter decreases from 73.7 to 65.3 nm with increasing sheath flow rate, which corresponds to an increase in the magnitude of the electric field. This figure clearly shows the alignment effect of electric field on mobility of rods. (Color figure available online.)

depends on the interaction energy between the particle and the external electric field.

In this work, we first compare the experimental mobility data with the mobility calculated from three regimes using our model

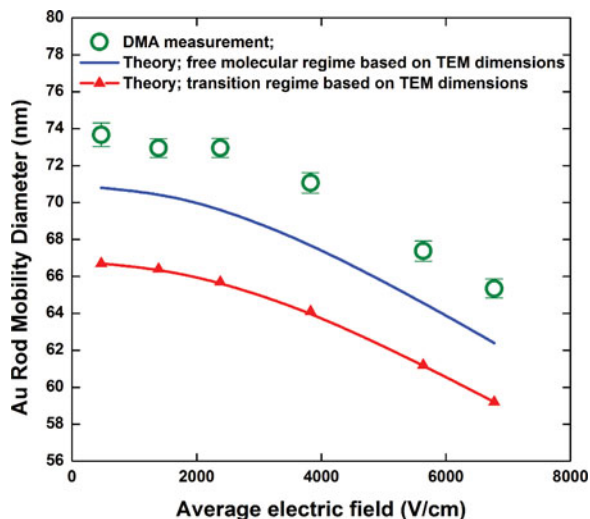


FIG. 4. Experimental measured mobility diameters for gold rods at various applied fields and compared with theoretical curves. The left two circles are measured mobility diameters at 0.833×10^{-4} m^3/s (5 L/min) and 2.5×10^{-4} m^3/s (15 L/min) using a long DMA, and the right four circles are measured values at 0.5×10^{-4} m^3/s (3 L/min), 0.833×10^{-4} m^3/s (5 L/min), 1.333×10^{-4} m^3/s (8 L/min), and 1.667×10^{-4} m^3/s (10 l/min) using a nano DMA. The theoretical curves of mobility diameter of a rod (diameter $d_r = 17$ nm and length $L_r = 270$ nm) plotted in the free molecular and transition regime. The finite diameter of the bath gas molecules, $d_g = 0.3$ nm, is considered by approximately increasing L_r and d_r by 0.3 nm (data from Ku and de la Mora 2009). (Color figure available online.)

with the rod dimensions determined by TEM image analysis (diameter $d_r = 17$ nm and length $L_r = 270$ nm). Second, assuming the dimensions of the gold rods are unknown, we show that by measuring the mobility as a function of applied field we can extract both the rod length and diameter using a nonlinear least square fit to the theory of Li et al. (2012).

3.2.1. Comparing Experimental Mobility with the Mobility Calculated in Three Regimes

The average electrical mobility of an axially symmetric particle in an electric field can be calculated based on our previous work (Li et al. 2012) (Equation (1) of Li et al. 2012),

$$\overline{Z}_p = q[K_{\perp}^{-1} + (K_{\parallel}^{-1} - K_{\perp}^{-1})\langle \cos^2 \theta \rangle], \quad [1]$$

where K_{\perp} is the principal component of the friction coefficient tensor perpendicular to the axial direction, K_{\parallel} is the component parallel to the axial direction, q is the net charge on the particle, and the $\langle \cos^2 \theta \rangle$ term arises due to the orientation distribution of particles.

Based on classical electrostatic theory, net charge for a conducting particle can be considered as distributed over the whole particle surface, regardless of field (Böttcher and Belle 1973; Jackson 1999). This implies that the net charge has no contribution to the particle alignment. An equivalent way to view this effect is to recognize that electron motion in a conductor is very fast. Further from Gauss's law, the field is pointing normal to the particle surface so that there is no component of the electric force tangent to the surface. This means there is no preferred location of the net charge on the surface and thus no torque from the net charge. In other words, while the electrophoretic velocity is net charge dependent, the actual orientation of the particle is not so. Thus, particle alignment is only determined by the polarizability and the randomization due to Brownian forces. Using the induced dipole polarization energy, (Equation (22) of Li et al. 2012), then the orientation is given by:

$$\langle \cos^2 \theta \rangle = \frac{1}{2\delta} \left[\frac{2\sqrt{\delta}e^{\delta}}{\sqrt{\pi}\text{Erfi}(\sqrt{\delta})} - 1 \right] \quad [2]$$

where $\delta = \frac{(\alpha_{\parallel} - \alpha_{\perp})E^2}{2kT}$, α_{\parallel} is the principal component of polarizability parallel to the axial direction, α_{\perp} is the component perpendicular to the axial direction, E is the electric field magnitude, k is the Boltzmann constant, T is the absolute temperature, and $\text{Erfi}(z) = \frac{2}{\sqrt{\pi}} \int_0^z e^{t^2} dt$, is the imaginary error function. Because no closed form expression for the polarization of a rod exists, Venermo and Sihvola (2005) reported a numerical study which showed that the polarizability of a rod is close to that of a spheroid with the same aspect ratio and permittivity. If we approximate, the polarization energy of a rod, with that of a prolate spheroid with the same volume, and the same aspect ratio as the rod, then α_{\parallel} and α_{\perp} is given by Equations (A13) and

(A14) in Li et al. (2012), with relative permittivity $\epsilon_k = \infty$ for a conducting particle (e.g., Au).

The friction coefficients, K_{\parallel} and K_{\perp} are given in Equations (A1) and (A2) in Li et al. (2012), for a rod in the free molecular regime, and given in Equations (A5) and (A6) in Li et al. (2012) for a slender rod in the continuum regime. Using Dahneke's scaling approach, the friction coefficient components for a particle in the transition regime can be expressed by the values of the friction coefficient components in the continuum regime and adjusted spherical diameters as

$$K_{\parallel, \text{transition}} = K_{\parallel, \text{continuum}} / C_c(d_{a, \parallel})$$

and

$$K_{\perp, \text{transition}} = K_{\perp, \text{continuum}} / C_c(d_{a, \perp}) \quad [3]$$

where the slip correction factor $C_c(d_p) = 1 + \frac{2\lambda}{d_p} [A_1 + A_2 \exp(-\frac{A_3}{2\lambda/d_p})]$, and $A_1 = 1.142$, $A_2 = 0.558$, $A_3 = 0.999$ is given by Allen and Raabe (1985) at room temperature $T = 296.15$ K and atmospheric pressure. The adjusted diameters are expressed by the mean free path of the gas molecules λ , the friction coefficient components in the continuum regime and in the free molecular regime as

$$d_{a, \parallel} = 2\lambda(A_1 + A_2)K_{\parallel, \text{freemolecular}} / K_{\parallel, \text{continuum}}$$

and

$$d_{a, \perp} = 2\lambda(A_1 + A_2)K_{\perp, \text{freemolecular}} / K_{\perp, \text{continuum}} \quad [4]$$

Using the expressions (Equations (1)–(4)) above, considering only the induced dipole polarization energy, we obtain theoretical curves for mobility diameter versus electric field for the gold rod with diameter 17 nm and length 270 nm in the three regimes in Figure 4. The finite diameter of the bath gas molecules, $d_g = 0.3$ nm, is considered by approximately increasing L_r and d_r by 0.3 nm (Ku and de la Mora 2009). The 4% uncertainty in the TEM measured width and length of gold, translates to ~ 2 –3 nm uncertainties in the theoretical mobility diameter in Figure 4, which means both theoretical curves can shift up or down in parallel 2–3 nm. This estimate includes the direct correlation between the length and width uncertainty. This 2–3 nm uncertainty is calculated from a change in mobility of a rod $d_r = 17$ nm and length $L_r = 270$ nm with at most a 4% change in dimension as determined from TEM. The variation of TEM dimensions roughly propagates linearly into a 4% uncertainty (2–3 nm/70 nm) in the mobility diameter which can be explained as for a slender rod in the free molecular regime the mobility diameter is roughly proportional to $(L_r \times d_r)^{1/2}$.

The mobility diameter calculated in the continuum regime is not shown in Figure 4, because it greatly overestimates the size of the rod (from 174–162 nm as electric field increases). The

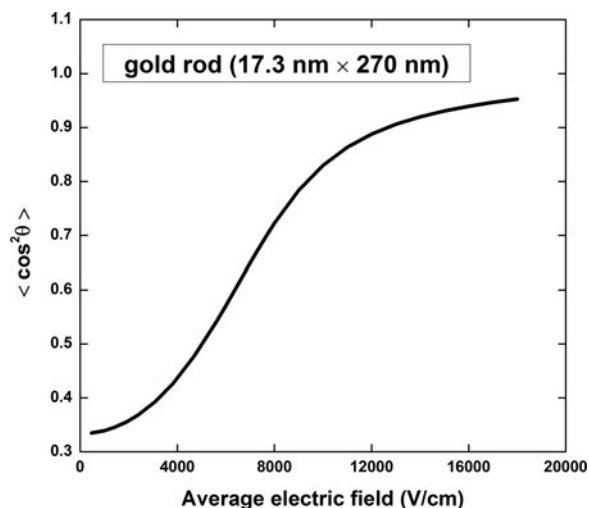


FIG. 5. Calculated $\langle \cos^2 \theta \rangle$ for the conducting rod ($d_r = 17$ nm; $L_r = 270$ nm) and considering the finite diameter of the bath gas molecules, $d_g = 0.3$ nm.

mobility diameter calculated in the free molecular regime shows the best fit to the experimental data, while values calculated in the transition regime (Daneke's adjusted spherical diameter approach) give a ~ 7 nm lower than experimental mobility. Since in this experiment, the rod length, $L_r = 270$ nm, is clearly in the transition regime, Figure 4 probably implies that the flow regime of a slender rod is most controlled by the diameter of the rod. In either case, both theoretical approaches show the same dependence of mobility (i.e., alignment) on electric field as the experimental data.

The calculated $\langle \cos^2 \theta \rangle$ for conducting gold rod ($d_r = 17$ nm; $L_r = 270$ nm) as a function of average field strength is shown in Figure 5. At low electric field, the value of $\langle \cos^2 \theta \rangle$ is close to the value at random orientation, $1/3$. As the intensity of electric field increases, the value of $\langle \cos^2 \theta \rangle$ increases toward the limit value of unity for a perfectly aligned rod.

3.2.2. Extracting Rod Length and Diameter from Mobility Measurements

Equation (1) shows that unlike a sphere there is more than one mobility for a given axially symmetric nonspherical particle, which implies that more than one dependent variable can be extracted from a well posed mobility study. Thus, the theory of Li et al. can be used (Equation (1)) to obtain shape information of an axially symmetric particle from mobility measurements. The friction coefficients, K_{\parallel} and K_{\perp} in Equation (1) are given in Equations (A1) and (A2) in Li et al. (2012), for a rod in the free molecular regime (where the gas viscosity, $\eta = 1.8325 \times 10^{-5}$ kg/m.s; the mean free path of gas, $\lambda = 67.3$ nm; the momentum accommodation, $f = 0.9$ used in this work) and $\langle \cos^2 \theta \rangle$ is given by Equation (2). The measured mobility versus electric field of our gold rods is plotted in Figure 6 showing how the mobility increases with increasing field, due to alignment. Evaluation and subsequent least-squares fitting is mathematically simplified by

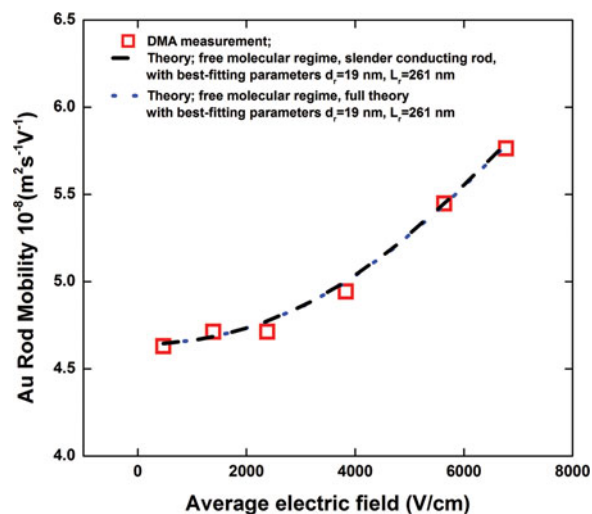


FIG. 6. Experimental measured mobility for gold rods (open squares [red]) at various applied fields, where the dimensions of the gold rods were determined by TEM ($d_r = 17$ nm and $L_r = 270$ nm). Black dashed line: nonlinear least-squares fit of Equation (1) with slender conducting rod approximation based on Equation (5) gives: $d_r = 19 \pm 0.2$ nm and $L_r = 261 \pm 8$ nm. Dotted (blue) line: full theory for rod, which is very close (the maximum deviation of mobility within the plot range is 0.16%) and overlapped with the slender approximation theory. (Color figure available online.)

making a slender conducting rod (length L_r , diameter d_r , aspect ratio $\beta = L_r/d_r \gg 1$) approximation for the values of polarizability in Equation (2),

$$\delta = \frac{(\alpha_{\parallel} - \alpha_{\perp})E^2}{2kT}, \quad \alpha_{\parallel} = \frac{\epsilon_0 \pi d_r^3 \beta^3}{4[\ln(2\beta) - 1]}, \quad \alpha_{\perp} = \frac{\epsilon_0 \pi d_r^3 \beta}{2}, \quad [5]$$

Here, ϵ_0 is free-space permittivity ($T = 296.15$ K used in this work). The deviation of δ for $\beta = 16$ between the value given by the slender approximation (5) and given by the full theory (Equations (A13) and (A14) in Li et al. 2012) is about 0.66%.

A nonlinear least-squares computer procedure (Wolfram Mathematica 8.0; FindFit () for $5 < d_r < 100$, $5 < \beta < 100$) was used to fit Equation (1), with the K_{\perp} and K_{\parallel} given in Equation (A1) and (A2) of Li et al. (2012) and the $\langle \cos^2 \theta \rangle$ given in Equations (2) and (5), to the mobility data in Figure 6. From this curve fitting procedure, the best values for diameter and length are $d_r = 19 \pm 0.2$ nm and $L_r = 261 \pm 8$ nm, which is in good agreement with the TEM measured rod dimensions, $d_r = 17$ nm and $L_r = 270$ nm. The theoretical curve using the full theory and the approximated theory based on Equation (5) with best-fitting parameters, $d_r = 19$ nm and $L_r = 261$ nm, are shown as the blue dotted line and black-dashed line in Figure 6. The slender rod approximation is very close to the full theory and the two theoretical curves are basically overlapped with each other. The rod diameter of the fitting result is off by $\sim 10\%$ compared with the TEM analysis, while the rod length is underestimated by $\sim 3\%$. One possible reason for this discrepancy is that these

gold rods do not fall exactly in the free molecular regime, thus not fully governed by Dahneke's drag force expression. An additional contribution to the discrepancy is the $\sim 4\%$ uncertainty of the TEM measurements.

4. CONCLUSIONS

Our general theory for the orientation-averaged mobility of a nonspherical particle in an electric field is applied to the specific case of a cylindrical particle. Theoretical results are compared with the experimental measurements of mobility of gold nanorods, with rod dimension determined by TEM images (width $d_r = 17$ nm and length $L_r = 270$ nm). The mobility size shift in the electric fields based on our model, expressed both in the free molecular regime and in the transition regime, shows the same trends as the experimental results but with a small offset. The experimental results are most closely fit assuming the rod is in the free molecular regime, as compared to the transition regime. Given that this rod has one dimension smaller than the mean free path and the other longer, implies that the flow regime of a slender rod is controlled by the diameter of the rod. As a demonstration of the application of our theory to extract shape information from a mobility measurement, we extract both the length and diameter of gold nanorods, which are found to be in good agreement with TEM analysis.

REFERENCES

- Allen, M. D., and Raabe, O. G. (1985). Slip Correction Measurements of Spherical Solid Aerosol-Particles in an Improved Millikan Apparatus. *Aerosol Sci. Tech.*, 4:269–286.
- Böttcher, C. J. F., and Belle, O. C. v. (1973). *Dielectrics in Static Fields*. Elsevier Scientific Pub. Co., Amsterdam, New York.
- Chan, P., and Dahneke, B. (1981). Free-Molecule Drag on Straight Chains of Uniform Spheres. *J. Appl. Phys.*, 52:3106–3110.
- Cheng, Y. S. (1991). Drag Forces on Nonspherical Aerosol-Particles. *Chem. Eng. Commun.*, 108:201–223.
- Dahneke, B. E. (1973a). Slip Correction Factors for Nonspherical Bodies—I Introduction and Continuum Flow. *J. Aerosol Sci.*, 4:139–145.
- Dahneke, B. E. (1973b). Slip Correction Factors for Nonspherical Bodies—II Free Molecule Flow. *J. Aerosol Sci.*, 4:147–161.
- Dahneke, B. E. (1973c). Slip Correction Factors for Nonspherical Bodies—III the form of the General Law. *J. Aerosol Sci.*, 4:163–170.
- Guha, S., Li, M., Tarlov, M. J., and Zachariah, M. R. (2012). Electro Spray-Differential Mobility Analysis of Bionanoparticles. *Trends Biotechnol.*, 30:291–300.
- Hinds, W. C. (1999). *Aerosol Technology: Properties, Behavior, and Measurement of Airborne Particles*. Wiley, New York; Chichester.
- Hubbard, J. B., and Douglas, J. F. (1993). Hydrodynamic Friction of Arbitrarily Shaped Brownian Particles. *Phys. Rev. E*, 47:R2983–R2986.
- Jackson, J. D. (1999). *Classical Electrodynamics*. Wiley, New York; Chichester.
- Kasper, G., Niida, T., and Yang, M. (1985). Measurements of Viscous Drag on Cylinders and Chains of Spheres with Aspect Ratios between 2 and 50. *J. Aerosol Sci.*, 16:535–556.
- Kim, S. H., Mulholland, G. W., and Zachariah, M. R. (2007). Understanding Ion-Mobility and Transport Properties of Aerosol Nanowires. *J. Aerosol Sci.*, 38:823–842.
- Kirkwood, J. G., and Riseman, J. (1948). The Intrinsic Viscosities and Diffusion Constants of Flexible Macromolecules in Solution. *J. Chem. Phys.*, 16:565–573.
- Kousaka, Y., Endo, Y., Ichitsubo, H., and Alonso, M. (1996). Orientation-Specific Dynamic Shape Factors for Doublets and Triplets of Spheres in the Transition Regime. *Aerosol Sci. Tech.*, 24:36–44.
- Ku, B. K., and de la Mora, J. F. (2009). Relation between Electrical Mobility, Mass, and Size for Nanodrops 1–6.5 nm in Diameter in Air. *Aerosol Sci. Tech.*, 43:241–249.
- Li, M. (2012). Quantifying Particle Properties from Ion-Mobility Measurements, in *Chemical Physics Program*, Dissertation, University of Maryland, College Park. Available online at: <http://hdl.handle.net/1903/13627>
- Li, M., Guha, S., Zangmeister, R., Tarlov, M. J., and Zachariah, M. R. (2011a). Quantification and Compensation of Nonspecific Analyte Aggregation in Electro Spray Sampling. *Aerosol Sci. Tech.*, 45:849–860.
- Li, M., Guha, S., Zangmeister, R., Tarlov, M. J., and Zachariah, M. R. (2011b). Method for Determining the Absolute Number Concentration of Nanoparticles from Electro Spray Sources. *Langmuir*, 27:14732–14739.
- Li, M., Mulholland, G. W., and Zachariah, M. R. (2012). The Effect of Orientation on the Mobility and Dynamic Shape Factor of Charged Axially Symmetric Particles in an Electric Field. *Aerosol Sci. Tech.*, 46:1035–1044.
- Li, M., Mulholland, G. W., and Zachariah, M. R. (2013). Mobility and Dynamic Shape Factors for Particle Doublets in Electric Fields. *Aerosol Sci. Tech.* (in review).
- Li, Z., and Wang, H. (2003). Drag Force, Diffusion Coefficient, and Electric Mobility of Small Particles. I. Theory Applicable to the Free-Molecule Regime. *Phys. Rev. E*, 68:061206.
- Mackowski, D. W. (2006). Monte Carlo Simulation of Hydrodynamic Drag and Thermophoresis of Fractal Aggregates of Spheres in the Free-Molecule Flow Regime. *J. Aerosol Sci.*, 37:242–259.
- Mason, E. A., and McDaniel, E. W. (1988). *Transport Properties of Ions in Gases*. Wiley, Hoboken, NJ.
- Shvartsburg, A. A., and Jarrold, M. F. (1996). An Exact Hard-Spheres Scattering Model for the Mobilities of Polyatomic Ions. *Chem Phys Lett.*, 261:86–91.
- Song, D. K., Lenggoro, I. W., Hayashi, Y., Okuyama, K., and Kim, S. S. (2005). Changes in the Shape and Mobility of Colloidal Gold Nanorods with Electro Spray and Differential Mobility Analyzer Methods. *Langmuir*, 21:10375–10382.
- Venermo, J., and Sihvola, A. (2005). Dielectric Polarizability of Circular Cylinder. *J. Electrostat.*, 63: 101–117.
- von Helden, G., Hsu, M. T., Gotts, N., and Bowers, M. T. (1993). Carbon Cluster Cations with up to 84 Atoms: Structures, Formation Mechanism, and Reactivity. *J. Phys. Chem.*, 97:8182–8192.
- Zhang, C. L., Thajudeen, T., Larriba, C., Schwartzentruber, T. E., and Hogan, C. J. (2012). Determination of the Scalar Friction Factor for Nonspherical Particles and Aggregates Across the Entire Knudsen Number Range by Direct Simulation Monte Carlo (DSMC). *Aerosol Sci. Tech.*, 46:1065–1078.
- Zelenyuk, A., and Imre, D. (2007). On the Effect of Particle Alignment in the DMA. *Aerosol Sci. Tech.*, 41:112–124.